

# Splitter for VLF and LF Applications

Whitham D. Reeve

---

## 1. Introduction

An RF signal *splitter* (also called *divider* or *power divider*) takes an input from an antenna or other signal source and directs it to two or more output paths for connection to test equipment or receivers. Important characteristics of a splitter are isolation of the output ports from each other, low insertion loss from input to output and impedance matching to prevent reflections.

A passive splitter also works in reverse as a *combiner* (or *power combiner*) to take two input signals and direct them to one output but the focus here is on its splitter function. This article describes a passive 2-way splitter (figure 1) for low frequency applications that may be shop-built and is intended for use between 10 and 100 kHz with a loop antenna and two low frequency receivers.

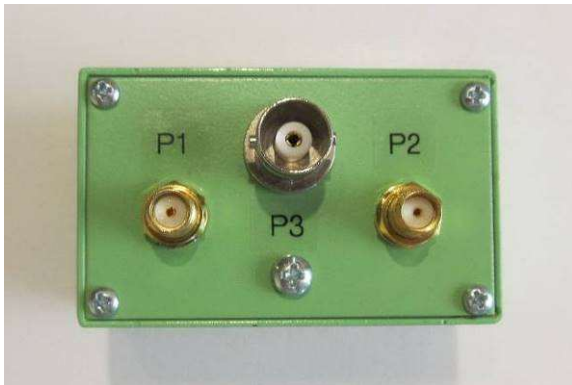


Figure 1 ~ Shop-built 2-way splitter ready for service. A signal connected to the BNC connector for Port 3 in the middle is split to SMA connectors for ports 1 and 2 on each side. The dimensions of the cast aluminum enclosure for this splitter are 2.25 L x 1.38 W x 1.13 H in (57 x 35 x 29 mm). Image ©2020 W. Reeve

---

## 2. Splitter Design & Construction

There are many RF splitter designs including resistor and transformer topologies. I decided to use a simple 3-port hybrid transformer topology that has a primary winding and bifilar wound, center-tapped secondary windings (figure 2). This topology provides outputs with 180° phase difference but this is of no consequence in my application. Three such 2-way splitters could be used as the basis for a 4-way splitter.

The impedance matching resistor in the secondary circuit is found from

$$R_s = R / (N_p / N_s)^2 \quad (1)$$

where  $R$  is the system impedance (50 ohms),  $R_s$  is the secondary matching resistance,  $N_p$  is the number of turns in the primary winding and  $N_s$  is the number of turns in each secondary winding. All impedances are assumed to be real (resistive). Eq. (1) may be derived using ordinary network analysis by noting that energy must be conserved from the input through the transformer to the outputs; alternately, see chapter 5 in the massive book [Kaiser] for a derivation. For equal impedances at all ports, the hybrid transformer requires a turns-ratio

$N_p/N_s = \sqrt{2} : 1 = 1.414:1$  from the primary to each secondary winding. Therefore, in a 50 ohm system,  $R_s = 50/2 = 25$  ohms.

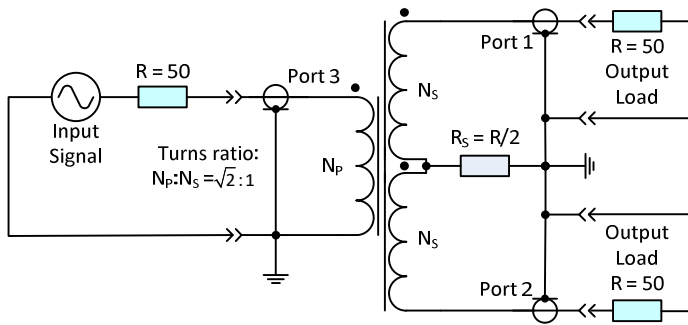


Figure 2 ~ Functional schematic of the 2-way splitter described in this article. A 50 ohm signal source is shown connected to port 3 on the left and 50 ohm terminations are shown connected to the output ports 1 and 2. The terminations represent receiver or test equipment loads. The system impedance is 50 ohms and denoted by the resistors labeled R. Resistor  $R_s$  connected to ground at the secondary center tap provides impedance matching. Note the winding polarity dots. Image ©2020 W. Reeve

The low frequency response ( $-3$  dB) of the splitter transformer may be determined from (see [Krauss])

$$f_{low}(Hz) = (R \cdot 10^9) / (4 \cdot \pi \cdot N_p^2 \cdot A_L) \quad (2)$$

where  $R$  and  $N_p$  have been defined previously, and  $A_L$  is the inductance factor in  $nH \text{ turns}^{-2}$  that takes into account the core material and its dimensional characteristics. The primary inductance  $L_p$  in  $nH$  may be substituted for the quantity  $N_p^2 \cdot A_L$ . The expected values for the primary and secondary inductances in  $\mu H$  are calculated from

$$L(\mu H) = A_L \cdot N^2 / 1000 \quad (3)$$

where  $N$  is the number of turns in the winding.

The bill of material for the splitter is simple (table 1). None of the parts are critical except the toroid core, which must be suitable for low frequency applications. I used a 75 mix toroid from Fair-Rite {FairRite}. Another possibility is the 76 mix from Fair-Rite but the available toroid sizes are limited. The wire size should be as large as possible yet still fit the core. Parts marked *generic* in the BOM were purchased through eBay or surplus suppliers or already in stock.

Table 2 ~ Bill of material for 2-way splitter

Description	Qty	Mfr	P/N
Enclosure, 2.25 L x 1.38 W x 1.13 H in	1	Pomona	2428
BNC-Female, solder cup, threaded panel mount	1	Generic	N/A
SMA-Female, solder cup, threaded panel mount	2	Generic	N/A
Turret terminal, insulated, 4-40 internal thread	1	Keystone	11512
Machine screw, 4-40 x 3/16 in, pan head	1	McMaster	90272A105
Washer, split lock, #4	1	McMaster	91101A005
Toroid core, low frequency mix	1	Fair-Rite	5975001101
Wire, 28 AWG, Kynar insulated, tinned copper	5 ft (1.5 m)	Generic	N/A

I used a Fair-Rite p/n 5975001101, EMI suppression toroid core with dimensions of 0.5 OD x 0.311 ID x 0.25 T in (12.70 x 7.90 x 6.35 mm) (figure 3). This ferrite core is made from manganese-zinc (MnZn) and has high relative permeability  $\mu$  (from the manufacturer's datasheet  $\mu = 5000$ ). Permeability indicates the ability of the material to

become magnetized when placed in a magnetic field; a high permeability is necessary to attain the high inductance required for low frequency applications.



Figure 3 ~ Fair-Rite toroid core, p/n 5975001101 (left) and toroid with primary and secondary windings of 28 AWG Kynar insulated wire (right). This image shows 24:17:17 windings, and each winding is a different color – violet for the primary and black and white for the two secondaries. Image ©2020 W. Reeve

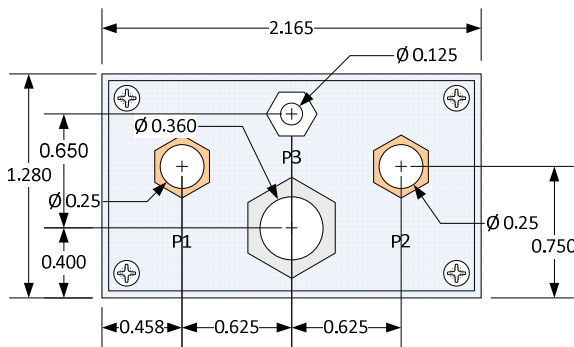


Figure 4 ~ Front panel drawing showing the dimensions and holes required for mounting the two SMA-F connectors, BNC-F connector and turret terminal. A blank panel is supplied with the Pomona enclosure that is used here. All dimensions are in inches. Image ©2020 W. Reeve

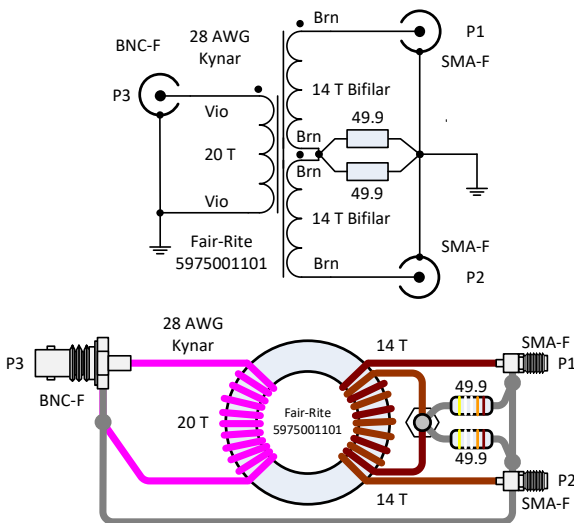


Figure 5 ~ Working schematic (upper) and wiring diagram (lower) for the 2-way splitter. The number of turns shown in the schematic and diagram are for the prototype; the final version used 24:17:17 turns. The diagram is conceptual. The bifilar secondary was parallel-wound first and the primary was then wound over it. I used two 49.9 ohm resistors in parallel for  $R_s$  and these together very closely approximate the required 25 ohms. An insulated turret terminal is used at the junction of  $R_s$  and the two secondary windings. Image ©2020 W. Reeve

Some suitable number of turns for the required primary:secondary:secondary turns ratio are 10:7:7, 14:10:10, 17:12:12, 20:14:14 and 24:17:17. The higher values provide better low frequency performance but the toroid core dimensions may be a limiting factor. I built two splitters, a prototype with 20 turns in the primary and 14 turns in each secondary winding and a final version with 24 primary turns and 17 secondary turns. From here on the two splitters are referred to as the *20:14:14 splitter* and the *24:17:17 splitter*, denoting the number of turns used.

The secondary is wound bifilar. In many inductor applications, the two wires used for a bifilar winding are twisted together before winding. This may be important at high frequencies where it is necessary to maintain transmission line effects in the winding [Krauss] but there is no apparent advantage at low frequencies (see the extensive experimental results described in [Sevick]). Therefore, I wound the two secondary wires physically in parallel around the toroid core (no crossovers), and then wound the primary wire over them.

Both windings in my transformers use 28 AWG Kynar insulated, tinned copper wire. To simplify identification, I used a different color insulation for each winding. Coated copper magnet wire and Litz wire also may be used and may allow more windings because of their smaller outside diameters. Larger wire sizes reduce losses due to skin effect, and a larger toroid core also may be used with a larger wire size to reduce losses. All else being equal, a larger core will allow more windings and lower frequency response.

The splitter is built in a small cast-aluminum enclosure with a removable panel drilled to hold the RF connectors (figure 4). The components are wired according to the working schematic and wiring diagram (figure 5) and assembly is simple (figure 6).

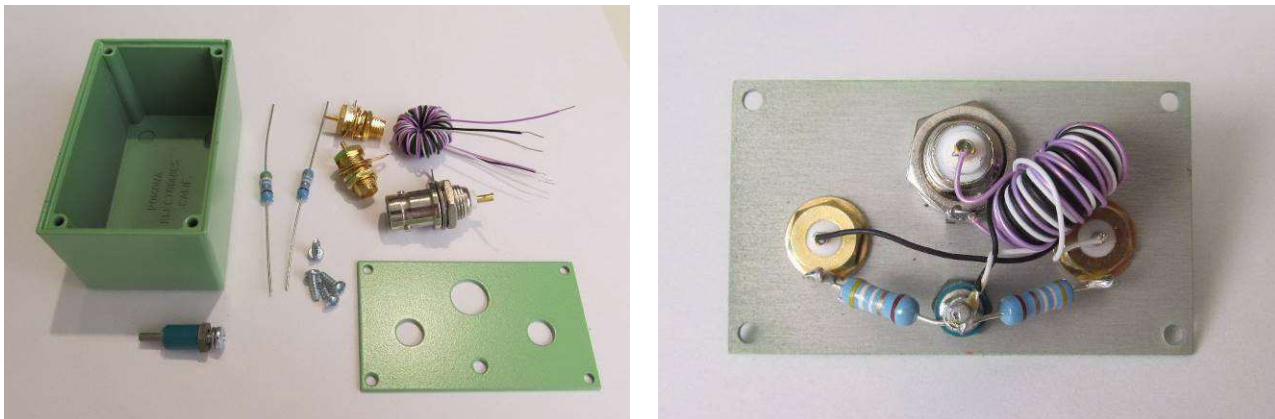


Figure 6 ~ Left: Splitter components ready for assembly after the enclosure was painted; Right: Splitter components installed on front panel. The transformer is on the right side between the BNC and right SMA connectors, and the resistors are connected from the turret terminal to the ground lug on each SMA connector. Image ©2020 W. Reeve

### 3. Measurements

For the Fair-Rite toroid used here,  $A_L = 3000 \text{ nH turns}^{-2}$  (specified in the manufacturer's datasheet at 10 kHz with a tolerance of  $\pm 20\%$ ). For comparison with the values calculated from eq. (3), I wound a transformer with 24:17:17 turns and then measured the inductance and Q of the windings with a Keysight U1733C LCR meter set to 10 kHz (table 2). The measured values are within 5 or 6% of the expected values.

The calculated and measured inductances discussed above are useful for design verification but they do not represent the splitter performance. The measurements that I conducted included the insertion loss between the input port (P3) and each output port (P1 and P2), the isolation between the two output ports and the return loss of each port. High isolation is necessary to ensure that the devices connected to ports 1 and 2 do not interact with each other, and high return loss indicates good impedance matching. Commercial splitter datasheets

usually include other parameters including phase and amplitude unbalance, but I am not particularly concerned about these so did not measure them.

Table 2 ~ Expected and measured winding inductances at 10 kHz for 24:17:17 core winding  
The  $\Delta$  column indicates the % change from the expected value

Color	Turns	Expected L (mH)	Measured L (mH)	Measured Q	$\Delta$
Black	17	0.867	0.914	71.7	+5%
White	17	0.867	0.914	71.5	+5%
Violet	24	1.728	1.837	64.6	+6%

For the splitter transformers described here, the  $f_{low}$  frequency calculated from eq. (2) for the 20:14:14 splitter is 3.3 kHz and for the 24:17:17 splitter is 2.3 kHz. For a 2-way splitter, the  $-3$  dB frequency response actually would be measured as  $-6$  dB at an output port because of the splitting loss. I measured the low frequency response by noting the frequency at which the insertion loss from port 3 to port 1 was 6 dB (includes the splitting loss). The measured frequencies were 3.2 kHz for the 20:14:14 splitter and 2.15 kHz for the 24:17:17 splitter, both of which are very close to the predicted values and significantly better than my required low frequency limit of 10 kHz.

Ideally, a 2-way splitter introduces a loss of exactly 3.01 dB between the input port and each output port but, in practice, the loss usually is a little higher due to core and winding losses and coupling inefficiency. This added loss typically is no more than about 0.5 dB, giving a total insertion loss  $< 3.5$  dB. The isolation between the output ports in an ideal splitter is infinite but is somewhat less in practical devices. Good quality commercial splitters have 20 to 30 dB or more isolation with 15 dB a typical minimum. The measurements discussed below may be compared to these *typical* values.

I used a VNWA-3E vector network analyzer and S-Parameter Test Set for all measurements (figure 7) (see [{Reeve2017}](#) for a description of this instrument combination). My measurements spanned 2 to 200 kHz, although my primary interest is 10 to 100 kHz. The VNWA-3E has a normal low frequency limit of 100 kHz, but by using special CoDec settings it can be extended much lower. For these measurements, I used 300 Hz sample rate and 1 x4 samples per IF period for a 75 Hz IF (rather than the default settings of 12 000 Hz sample rate and 48 000 Hz IF). The splitter insertion loss and isolation is represented by scattering parameter transmission coefficients S21 and S12 and the return loss is represented by reflection coefficients S11 and S22. All parameters are displayed in dB from 5 to 200 kHz.

My S-Parameter Test Set has SMA connectors so I used short (12 in, 300 mm) jumper cables with SMA-M connectors on one end for connection to the test set and BNC-M on the other for connection to the splitter. I set the software for 1001 sweep frequency points (frequency resolution of 198 Hz) and calibrated the VNA at the end of these cables with an SDR-Kits *BNC Calibration Kit*. I used BNC-F to SMA-M adapters for connection to the output ports and assumed the adapters have negligible effect at the low frequencies used in the measurements.

The insertion loss, return loss and isolation measurements yielded good results with no surprises (figures 8 and 9). Marker tables are shown in the upper-left corner of each plot that tabulate the performance at specific frequencies. There were no discernible differences between the two output ports on the 20:14:14 splitter but one port on the 24:17:17 splitter was slightly better than the other. For both splitters, the insertion loss is better

than 3.5 dB at 10 kHz and improves to near-ideal values of 3.0 dB above 10 kHz. The 24:17:17 splitter is slightly better at 10 kHz than the 20:14:14 splitter.

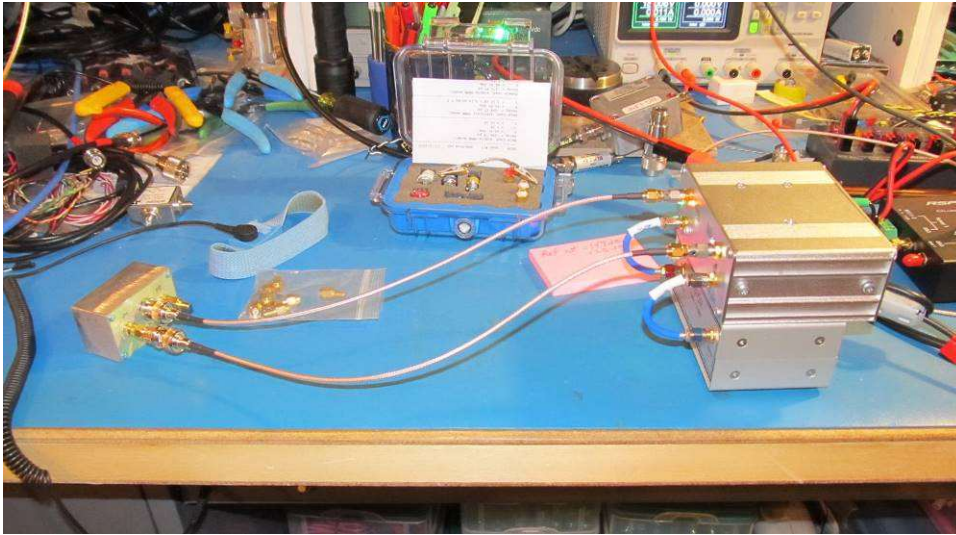


Figure 7 ~ Low frequency splitter prototype on the bench (at left) connected to the VNWA-3E vector network analyzer with shop-built S-Parameter Test Set (right). The two jumper cables on the S-Parameter Test Set are made from RG-316 coaxial cable and are 150 mm long. The BNC calibration kit is visible in the middle-background. ©2020 W. Reeve

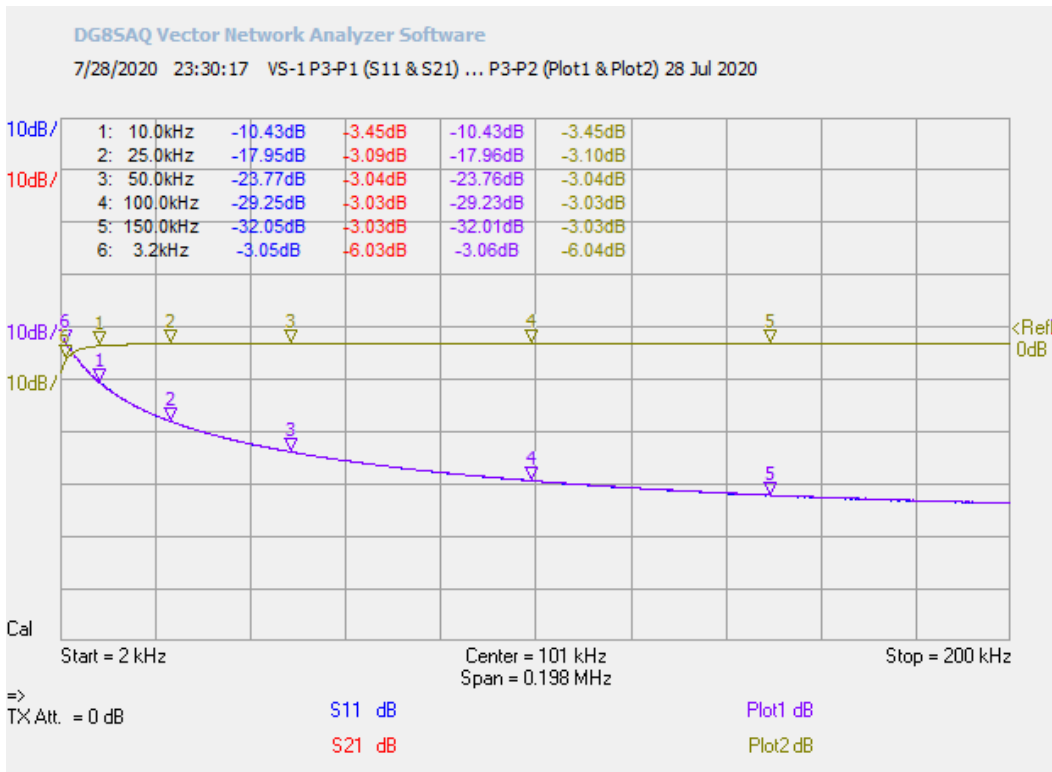


Figure 8.a ~ Insertion loss and return loss measurements over the frequency range 2 to 200 kHz for the 20:14:14 splitter. The insertion losses from the input port P3 to output ports P1 and P2 are shown by the red/green traces labeled S21 and Plot 2, respectively. The return losses for port P3 are shown by the blue/violet traces labeled S11 and Plot1.

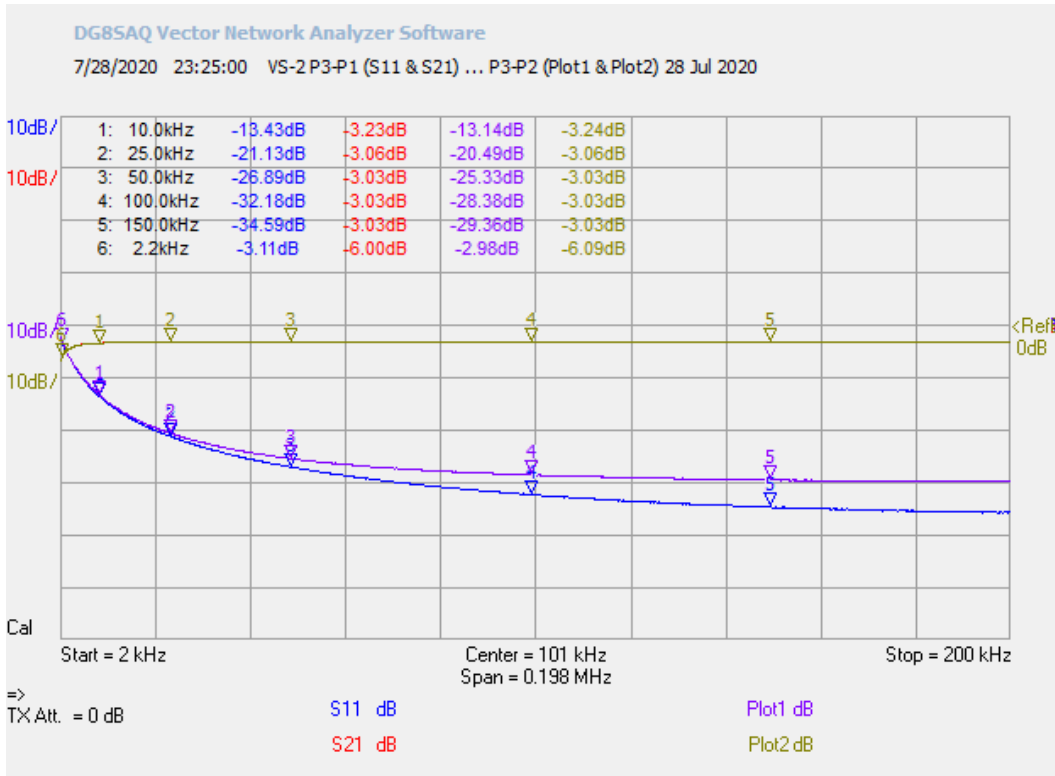


Figure 8.b ~ Insertion loss and return loss measurements over the frequency range 2 to 200 kHz for the 24:17:17 splitter. The insertion losses from the input port P3 to output ports P1 and P2 are shown by the red/green traces labeled S21 and Plot 2, respectively. The return losses for port P3 are shown by the blue/violet traces labeled S11 and Plot1.

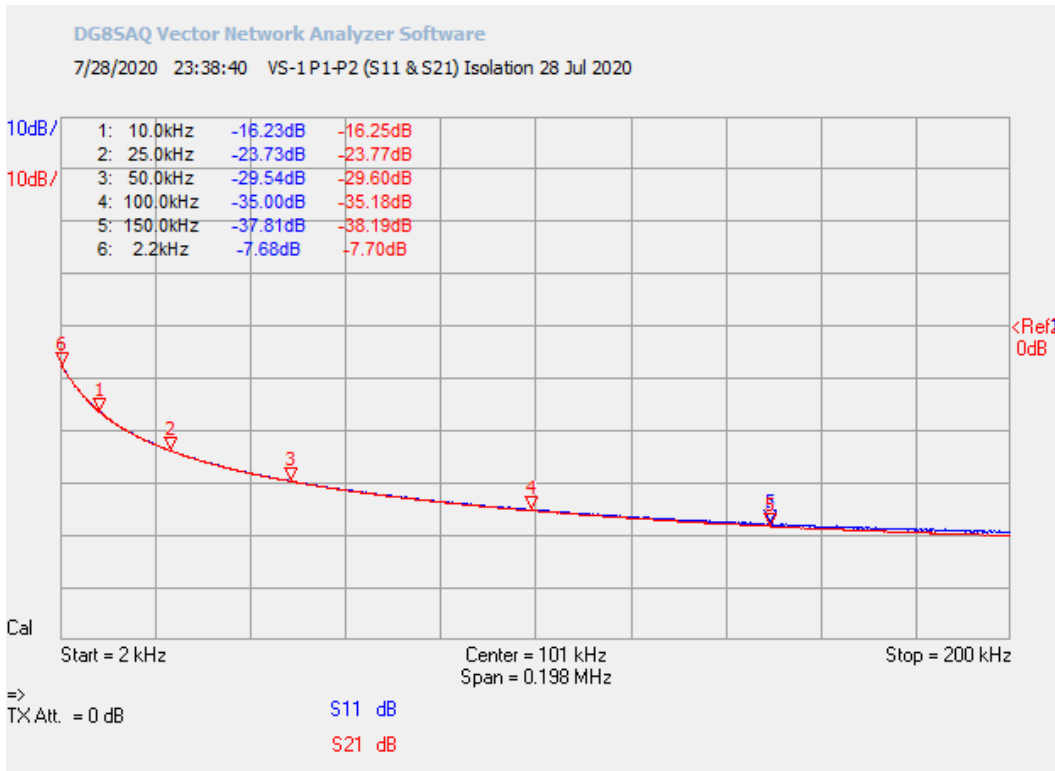


Figure 9.a ~ Isolation measurements between output ports P1 and P2 with input port P3 terminated for the 20:14:14 splitter. The isolation worsens at the lower measurement frequencies but still is better than a typical requirement of 15 dB. The isolation increases to better than 35 dB at 100 kHz.

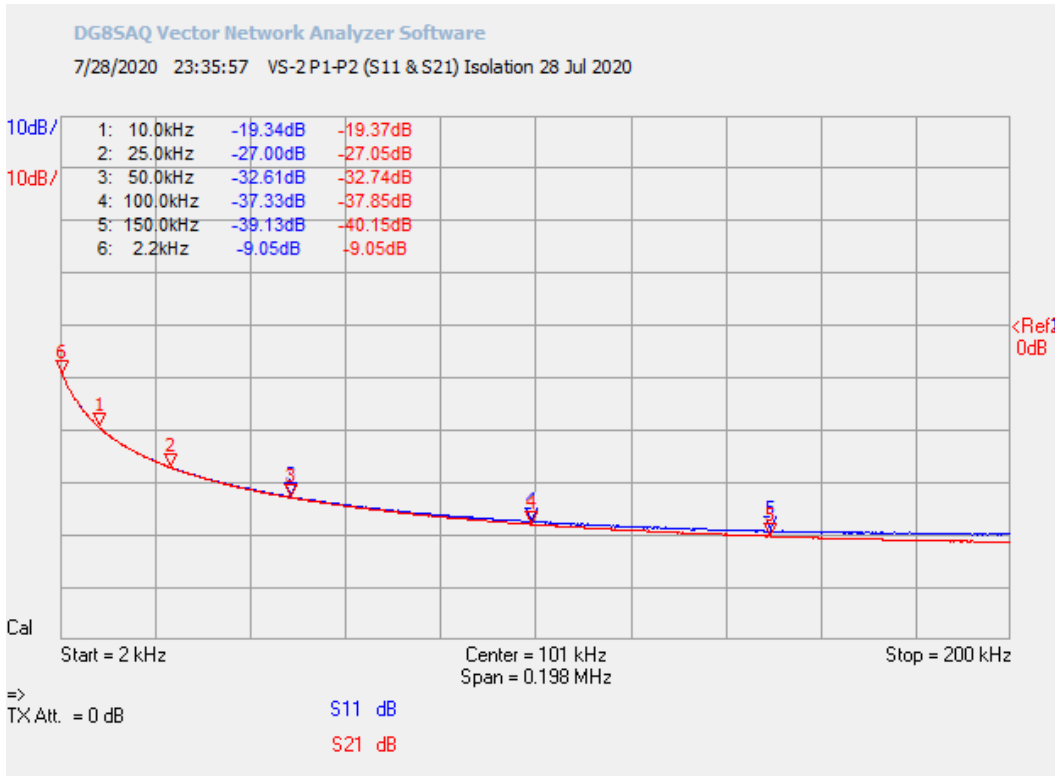


Figure 9.b ~ Isolation measurements between output ports P1 and P2 with input port P3 terminated for the 24:17:17 splitter. The isolation worsens at the lower measurement frequencies but still is better than a typical requirement of 15 dB. The isolation increases to better than 35 dB at 100 kHz. As with insertion loss and return loss, the isolation of the 24:17:17 splitter is marginally better.

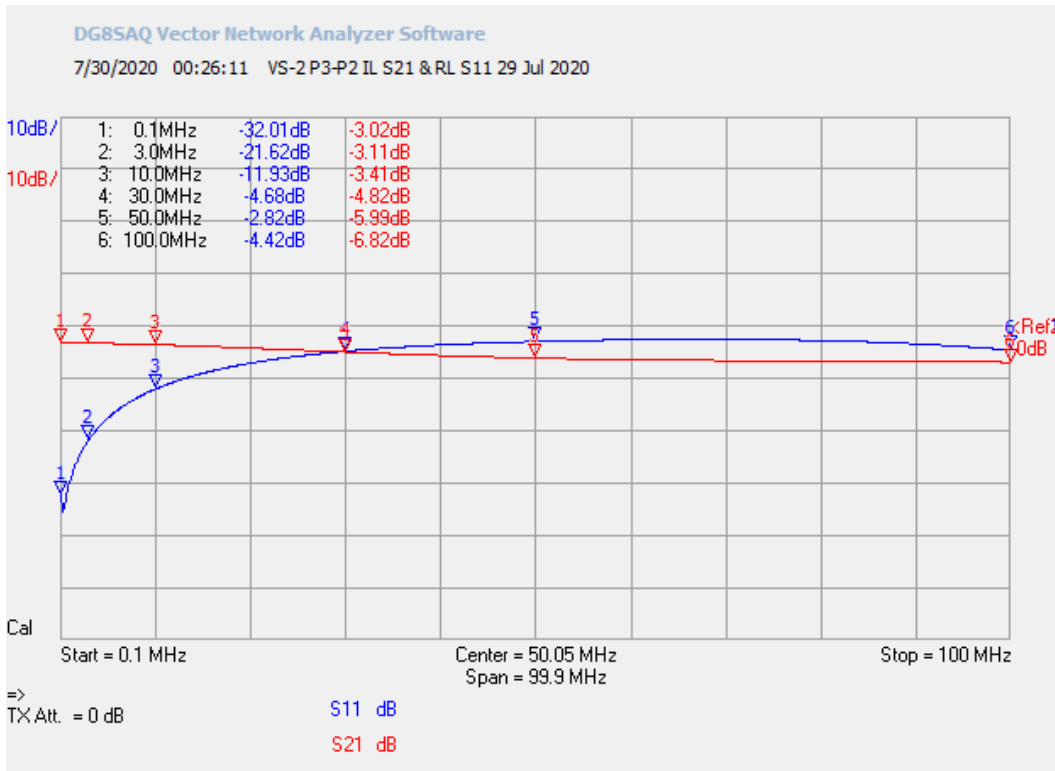


Figure 10.a ~ Insertion loss and return loss measurements over the frequency range 0.1 to 100 MHz for the 24:17:17 splitter. The insertion loss from the input port P3 to output port P2 is shown by the red trace labeled S21. The return loss for port P3 is shown by the blue trace labeled S11. The insertion loss at 10 MHz is 3.4 dB.

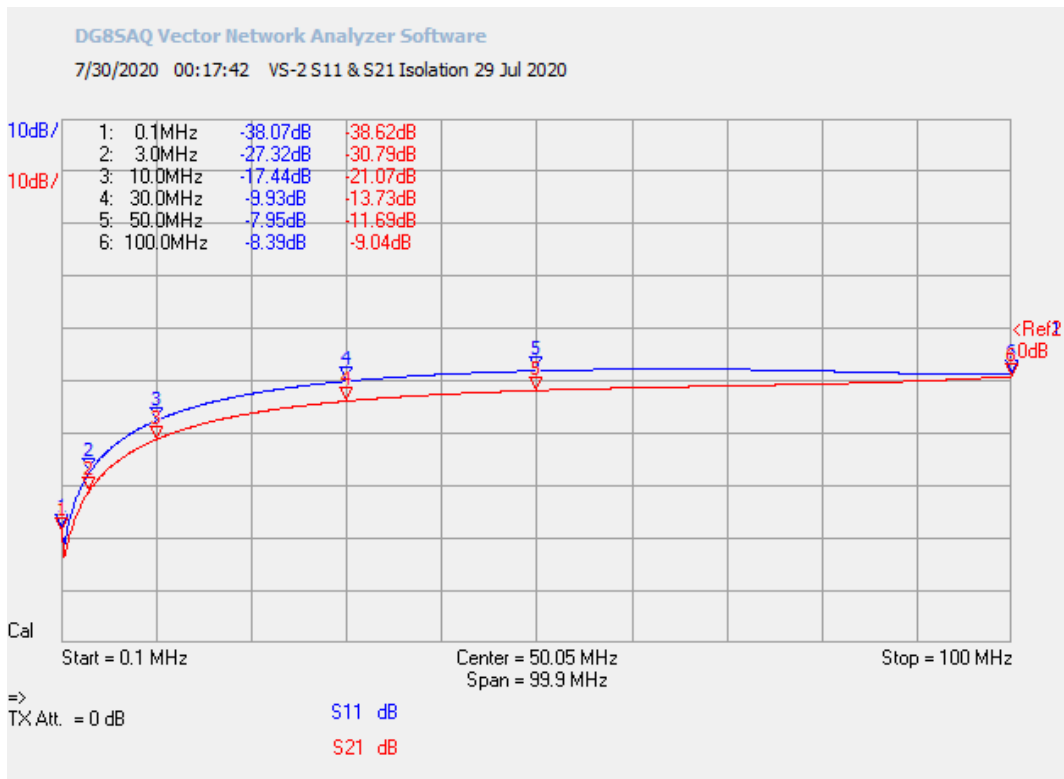


Figure 10.b ~ Isolation measurement for the 24:17:17 splitter between output ports P1 and P2 with input port P3 terminated. The isolation worsens at the higher measurement frequencies but still is better than 20 dB at 10 MHz.

The return loss of the 20:14:14 splitter at 10 kHz is acceptable at 10.4 dB (equivalent to VSWR = 1.9) and it steadily improves to 29.2 dB at 100 kHz (equivalent to VSWR = 1.07), whereas the 24:17:17 splitter is approximately the same on one port but a few dB better on the other port. Isolation in the 20:14:14 splitter is 16.2 dB at 10 kHz, increasing to 35.0 dB at 100 kHz, and the 24:17:17 splitter is about 3 dB better. The marginally better performance of the 24:17:17 splitter compared to the 20:14:14 could be for any number of reasons but is statistically irrelevant because only one of each transformer was built.

In addition to the measurements up to 200 kHz described above, I also made a set of measurement from 100 kHz to 10 MHz (figure 10). The frequency resolution was 99.8 kHz, and I recalibrated the VNWA-3E with the default CoDec values. I was not expecting much, mainly because the permeability of the 75 mix cores drops rapidly above 1 MHz. The two splitters were approximately the same in their degradation with increasing frequency.

If the insertion loss is to be limited to 3.5 dB, it looks like the splitters are usable to 10 MHz or so. The return loss at that frequency decreased to about 12 dB. I noticed that the insertion loss of the two ports diverged above 10 MHz with one port on each splitter showing more loss. This may be due to the asymmetric mounting of the transformer that caused the lead for one of the output ports to be longer than the other or the physical relationships of the transformer windings distorting the coupling. As for the isolation between the two output ports, it decreases with increasing frequency but still is over 20 dB at 10 MHz.

## 4. Conclusions

A low frequency, hybrid transformer, RF splitter is described that uses a high-permeability ferrite toroid core wound with insulated wire. Measurements with a vector network analyzer show the insertion loss from the input to output ports is nearly the ideal 3 dB throughout the desired frequency range 10 to 100 kHz, the isolation is better than 16 dB at 10 kHz and rising to above 35 dB at 100 kHz and the return loss is better than 10 dB (equivalent to VSWR = 1.9) at 10 kHz, rising steadily to almost 29 dB (equivalent to VSWR = 1.07) at 100 kHz. Two splitters were built, one with 20:14:14 transformer windings and the other with 24:17:17 windings. The transformer with the higher number of windings had slightly better performance.

---

## 5. Weblinks and References

{FairRite} <https://www.fair-rite.com/product-category/inductive-components/toroids/high-permeability-75-ui5000-material/>

[Kaiser] Kaiser, K., Electromagnetic Compatibility Handbook, CRC Press, 2005

[Krauss] Krauss, H. and Allen, C., Designing Toroidal Transformers to Optimize Wideband Performance, Electronics, August 16, 1973

{Reeve2017} Reeve, W., Building Version 2 of an S-Parameter Test Set for the VNWA-3E, 2017, available at: [http://www.reeve.com/Documents/Articles%20Papers/Reeve\\_S-ParamTestSet\\_V2.pdf](http://www.reeve.com/Documents/Articles%20Papers/Reeve_S-ParamTestSet_V2.pdf)

[Sevick] Sevick, J., Transmission Line Transformers, 4<sup>th</sup> ed., Noble Publishing Corp., 2001

---



Author: Whitham Reeve is a contributing editor for the SARA journal, Radio Astronomy. He obtained B.S. and M.S. degrees in Electrical Engineering at University of Alaska Fairbanks, USA. He worked as a professional engineer and engineering firm owner/operator in the airline and telecommunications industries for more than 40 years and now manufactures electronic equipment used in radio astronomy. He has lived in Anchorage, Alaska his entire life. Email contact: [whitreeve@gmail.com](mailto:whitreeve@gmail.com)

---

**Document information**

Author: Whitham D. Reeve

Copyright: © 2020 W. Reeve

Revision: 0.0 (Original draft started, 23 Jul 2020)  
0.1 (Added images and measurements, 24 Jul 2020)  
0.2 (Completed 1<sup>st</sup> draft, 25 Jul 2020)  
0.3 (Updated some images, 26 Jul 2020)  
0.3 (Added 10 MHz measurements, 29 Jul 2020)  
0.4 (Revised figure 2, 05 Sep 2020)

Word count: 1974

File size: 324096